Incorporating Noise Quantitatively in the Phase Field Crystal Model via Capillary Fluctuation Theory

Gabriel Kocher,[1] Nana Ofori-Opoku,[2,3] and Nikolas Provatas[1]
[1]Department of Physics, Centre for the Physics of Materials, McGill University, Montreal, Quebec H3A 2T8, Canada
[2]Materials Science and Engineering Division, National Institute of Standards and Technology, Gaithersburg, Maryland 20899, USA
[3]Center for Hierarchical Materials Design, Institute of Science and Engineering, Northwestern University, Evanston, Illinois 60208, USA

(Received 12 July 2016; published 23 November 2016)

A tacit assumption underlying most phase field models of nonequilibrium phase transformations is that of scale separation. Stochastic order parameter field theories utilize noise to separate atomic-scale fluctuations from the slowly varying fields that describe microstructure patterns. The mesoscale distribution of such stochastic variables is generally assumed to follow Gaussian statistics, with their magnitude following fluctuation-dissipation relations. However, there is still much debate about how atomic-scale fluctuations map onto the mesoscale upon coarse graining of microscopic theories. This Letter studies interface fluctuations in the phase field crystal (PFC) model and proposes a self-consistent method for relating how the effective noise strength and spectral filtering of the noise in the PFC model, and similar types of microscopic models, should be defined so as to attain the spectrum of mesoscale capillary fluctuations quantitatively.

DOI: 10.1103/PhysRevLett.117.220601

The properties of most materials are known to be strongly correlated to the internal structure between the nanometer to micrometer scales. For example, the strengthening and plastic deformation of metals is controlled by the patterning of grain boundaries, multiphase boundaries, dislocation density, and impurity atoms. In semiconductors, the band structure is strongly modified by the presence of all the aforementioned defects. The microstructure in solids is established at the time of solidification and subsequently modified by various thermal and mechanical processes. All these processes are nonequilibrium phase transformations that govern the arrangement of atoms across multiple scales. As such, the ability to control and manipulate microstructure in order to design materials with desired properties translates to a need for experimentally characterizing and theoretically modeling microstructure across many scales.

In the study of nonequilibrium phase transformations relevant to materials, it is crucial to capture and integrate atomic-scale features into mesoscale phase field theories, which are well known to be thermodynamically consistent at long length and time scales. Toward this goal, phase field crystal (PFC) modeling [1,2] has recently emerged as an efficient and mathematically accessible methodology that integrates the thermodynamics of phase transformations with many salient solid- and liquid-state properties emergent at the atomic scale, including elastoplastic deformation, grain boundaries, rotational grain invariance, and nucleation, all on diffusive time scales [3]. Extensions to the original PFC model have been developed to model complex structural transformations in pure materials [4–6], multicomponent alloys [7–10], and the study of solidification and solid-state transformations [11–13].

There has been much debate in the modeling community about the fluctuations in the PFC model [14]. One approach, motivated through classical density functional theory (cDFT), argues that the density field evolved is an ensemble averaged quantity. This description suggests that the use of a stochastic noise term is inconsistent, as it would lead to double counting temperature effects. On the other hand, although the PFC order parameter is formally related to the cDFT density, it retains only its salient features, making PFC modeling a paradigm of its own. If one rather interprets the PFC density as a temporally coarse-grained quantity, one should add a stochastic term to the density equation to account for effects faster than the coarse-graining time scale. This addition is particularly important to allow the system to overcome energy barriers required to emulate nucleation in solidification or grain depinning in solid-state transformations, to name but a few effects.

Noise in traditional phase field type models and PFC is generally assumed to be of the Langevin type, following fluctuation dissipation in the bulk. This makes it possible to identify the stochastic noise amplitude when the model is mapped to a specific material through the various expansion parameters in the free energy. In its more popular form, however, the PFC model is cast into reduced, dimensionless units, a form that treats some of the expansion parameters as variables. In this paradigm, under what conditions does the PFC theory follow the long-wavelength behavior predicted by statistical mechanics? Moreover, different coarse-graining approaches used to attain the long-wavelength

 © 2016 American Physical Society

limit typically introduce approach-specific scale factors in the free energy and the effective coarse-grained noise variables [15–20]. As a result, it is not clear how the application of noise at the microscopic PFC scale modulates the model's mesoscale predictions. A long-standing question therefore remains to be answered: Since PFC noise accounts for effects washed out by the temporal coarse-graining procedure, what spatial distribution and magnitude should it have so that PFC theory quantitatively reproduces the long-wavelength behavior predicted by statistical mechanics?

Another key question is that of noise filtering. While it is clear that all continuum models require an addition of noise to create capillary fluctuations, it is not obvious that introducing noise at shorter length scales than the interface width does not overcount temperature effects at the mesoscale. Unfiltered noise induces a divergence of the noise-induced excess potential [21], which is why several authors have introduced a high-k noise cutoff [3,22–24]. Numerically, the grid spacing naturally sets a cutoff length scale; however, this is much shorter than the typical scales at play in the simulation. It has also been suggested that the noise-induced excess potential should be on the order of the potential barrier, which leads to a cutoff around the interatomic length scale [21].

In this Letter, we examine interface fluctuations in the PFC model in the context of long-wavelength capillary fluctuation theory in order to determine a self-consistent relationship between the microscopic PFC noise and the emergent fluctuations at the mesoscale. The approach described here can be applied to any type of continuum theory. The specific application here to the PFC model allows us to fix the stochastic PFC noise strength unambiguously as a function of this model's free energy parameters. In this example, we also demonstrate that the cutoff in noise filtering is crucial for attaining a quantitative match with capillary fluctuation theory. To our knowledge, this is the first attempt to establish a method for fixing the strength of the PFC noise to be fully self-consistent with the correct long-wavelength behavior.

We consider the following PFC dynamical equation:

$$\partial_t n(\mathbf{r}) = \Gamma\nabla^2 \frac{\delta\mathcal{F}[n(\mathbf{r},t)]}{\delta n(\mathbf{r},t)} + \eta(\mathbf{r}), \tag{1}$$

where $\mathcal{F} = F/(\bar{\rho}R^d k_B T)$ is the dimensionless PFC free energy [1,3], given by

$$\mathcal{F} = \int d\mathbf{r}\left(\frac{n}{2}[\Delta B + B_x(1+\nabla_r^2)^2]n - \frac{n^3}{6} + \frac{n^4}{12}\right), \tag{2}$$

where $n(\mathbf{r})$ is the microscopic PFC order parameter field, η is a stochastic noise term, and Γ is the atomic mobility. Here T is the temperature, k_B is the Boltzmann constant, $\bar{\rho}$ is a reference density (which serves as an expansion point of the theory), R is a characteristic length scale, and d is the dimensionality of the system. In this model, ΔB acts as an effective temperature, and B_x is the bulk compressibility of the solid phase, which allows for the modeling of different types of materials and interfaces. For a fixed value of ΔB, large B_x values will result in metalliclike diffuse interfaces, while smaller values of B_x yield polymerlike atomically sharp interfaces.

Assuming completely uncorrelated events on short length and time scales, η is assumed to follow Langevin-type dynamics, i.e., be a Gaussian stochastic noise variable satisfying the form

$$\langle\eta(\mathbf{r},t)\eta(\mathbf{r}',t')\rangle = -N_a^2\nabla_c^2\delta(\mathbf{r}-\mathbf{r}')\delta(t-t'), \tag{3}$$

where N_a^2 is the amplitude of the noise. The index "c" in ∇_c^2 indicates a possible cutoff to the scale of the noise (discussed below). For the case of $\eta(\mathbf{r}) = 0$, the functional of Eq. (2) allows for the simulation of the equilibrium properties of interfaces, such as their surface energies [17–20,25,26]. Such interfaces, however, do not fluctuate and cannot be spontaneously generated from the bulk through nucleation events. Conversely, with $\eta(\mathbf{r}) \neq 0$, several works have shown that noise allows for the phenomenology of nucleation of nonequilibrium solid precursors [22], depinning, and step growth [16].

It can be shown that bulk fluctuations establish the noise amplitude in the form $N_a^2 = 2\Gamma/\bar{\rho}R^d$. In theory, matching the model to a specific phase space of a given material should provide the values for $\bar{\rho}$, R, and Γ. For example, taking R to be the lattice constant of the crystal would make the product $\bar{\rho}R^d$ the number of atoms per unit cell. However, here we show that, in order to recover the long-wavelength capillary fluctuation spectrum of a solid-liquid interface quantitatively, the product $\bar{\rho}R^d$ must in fact be fixed in a way that depends on the parameters of the free energy functional.

Statistical mechanics predicts that capillary fluctuations of a solid-liquid interface must obey $\langle|A|^2 f\rangle = 1/L^{d-1}(k_B T)/(\gamma+\gamma'')1/K^2$, where A is the amplitude of the Fourier mode with wave vector K, γ is the surface energy, γ'' is its second derivative with respect to orientation ($\gamma+\gamma''$ is called the surface stiffness), and L^{d-1} is the length (2D) or area (3D) of the fluctuating structure. Hoyt and co-workers have shown [27,28] that this equation also describes the mesoscale behavior of interfaces simulated through molecular dynamics. Tóth, Gránásy, and Tegze also showed that the $1/K^2$ form also emerges in PFC simulations [29]. The expression for $|A|^2$ has units of m^{d-1}. Scaling to PFC units ($\mathbf{k} = \mathbf{K}R$, $\tilde{L} = L/R$) and introducing $\tilde{\gamma} = \gamma/(k_B T\bar{\rho}R)$ yields

$$\langle|\tilde{A}|^2\rangle \equiv \langle|A|^2\rangle\bar{\rho}R = \frac{1}{\tilde{L}^{d-1}}\frac{1}{\tilde{\gamma}+\tilde{\gamma}''}\frac{1}{k^2}, \tag{4}$$

which is dimensionless since $[\bar{\rho}R] = 1/m^{d-1}$. It is noteworthy that the rescaled capillary fluctuation spectrum (4)

depends only on rescaled variables of our model and can thus be related quantitatively to results obtained directly from PFC simulations. In what follows, we first perform simulations of a solid-liquid interface with $\eta(\mathbf{r}) = 0$ from an amplitude formulation (so-called phase field limit) of the PFC energy of Eq. (2) and extract the interface stiffness. This is done by subtracting the total grand potential energy of the system from the grand potential of the bulk based on standard approaches [17,26]. The amplitude formulation used here is analogous to that developed by Majaniemi and Provatas [18,20]. Using the full atomistic PFC model, we then perform simulations where we fluctuate the interface with different N_a values and with different spatial cutoffs of the noise spectrum. In each case, we compute $\langle|\tilde{A}|^2\rangle$ and use Eq. (4) as a target theory from which to extract the correct value of N_a^2 in Eq. (3).

A PFC simulation box of 1000×4000 grid points is setup with a single slab of solid filling the box in the $\hat{y}$ direction and where one of the triangular basis vectors of the solid phase is pointed along the $\hat{y}$ direction. The slab dimensions are ~60 layers × 400 atoms. The slab is surrounded by liquid and the model parameters set to be in the middle of the coexistence region of the phase diagram. The interface runs along the $\hat{y}$ direction (see Fig. 1). The rescaled PFC model (1) and (2) is evolved using a semi-spectral Fourier space algorithm with a time step of 1 in dimensionless units. The position of the interface is detected with an atomic peak tracker, with entry into the bulk solid being identified as soon as the peaks of $n(\mathbf{r})$ exceed the average value $(n_{\text{solid}} + n_{\text{liquid}})/2$. Here n_{liquid} and n_{solid} are the equilibrium densities of the two phases, as measured in a noiseless environment. We first perform 10^6 time steps to allow the interface to reach a stationary state, before recording its evolution for another 3×10^6 time steps. In averaging interface configurations over time, care is taken to account for self-correlations of the interface at different wavelengths. This is reflected in the error bars shown, and details are provided in Supplemental Material [30]. To collect independent statistics, ten different runs are performed and the power spectra averaged.

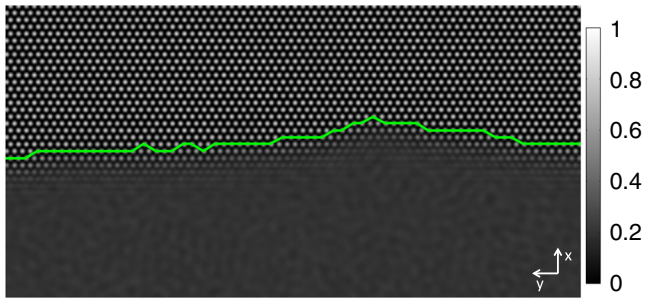

FIG. 1. Sample PFC density field of coexisting solid and liquid phases. $B_x = 0.55$, $\Delta B = 0.18$, and $N_a = 0.04$. The green line joins the atomic peaks defining the detected interface. This picture shows ~1/3 and ~1/6 of the simulation box in $\hat{x}$ and $\hat{y}$, respectively.

Some sample interface power spectra are presented in Fig. 2. Here $B_x = 0.55$, $\Delta B = 0.18$, and $n_o = 0.207$. Single (black) lines show the interface spectrum, averaged over time and ten different runs. The color regions show the envelope of the error bars. Using Eq. (3) without filtering, we obtain the red line in the figure. While a power law is obtained, comparing to the expected $1/k^2$ spectrum (dashed red line), we see a notable discrepancy. We suspect nonlinear cross mode coupling is responsible for this modification. This deviation can be corrected by removing modes with $k > k_{\max}$. If $k_{\max} \leq k_\lambda$, with k_λ the k mode corresponding to the crystal wavelength, the spectrum changes to the correct $1/k^2$ scaling. This behavior is robust, since any value of $k_\lambda/k_{\max}$ we have chosen between 1 and 5 yields the same result. A slight power loss on the order of the atomic length scale was seen with $k_\lambda/k_{\max} = 10$ (not shown for clarity). To our knowledge, this is the first demonstration showing that noise filtering is necessary to account for fluctuations in the correct way in PFC simulations. We expect that, without filtering, $1/k^2$ scaling will be achieved at very low k values; however, these are typically beyond the range of practical PFC simulation systems.

With a methodology for establishing a noise cutoff in hand, we proceed to study the prefactor multiplying $1/k^2$ in Eq. (4). All simulations presented here use the value $k_\lambda/k_{\max} = 1.5$. We start by examining its scaling with the amplitude of the noise. Following Ref. [16], one can analytically determine the interface fluctuations from the PFC model, through the amplitude formalism and interface projection technique. This results in the expression

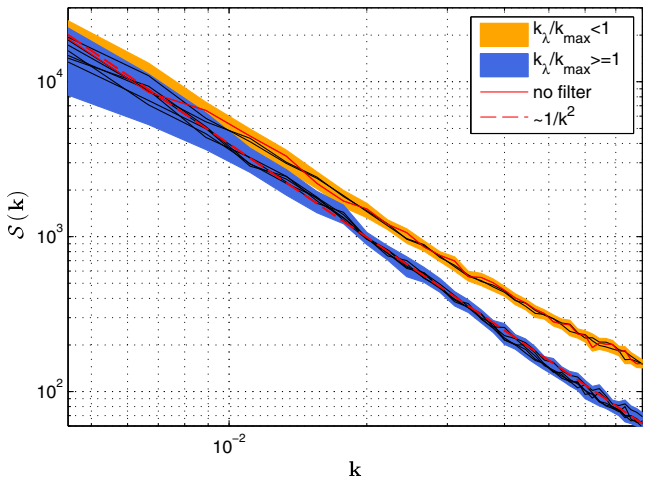

FIG. 2. Power spectra of a fluctuating interface for different noise cutoff wave vectors $k_{\max}$ (solid curves in black and red). The error bar envelopes corresponding to the solid curves with $k_\lambda/k_{\max} = 0$, 0.5, 0.75 are highlighted in yellow, while those for $k_\lambda/k_{\max} = 1$, 1.25, 1.5, 2, and 5 are highlighted in blue. The red dashed line shows $1/k^2$. For reference, $k = 10^{-2}$ is the wavelength corresponding to roughly 90 atomic lengths.

$$\langle|\tilde{A}|^2\rangle = \frac{1}{\tilde{L}^{d-1}}\frac{N_a^2}{\mathcal{S}k^2}, \tag{5}$$

where $\mathcal{S}/N_a^2$ is an effective dynamical stiffness of the model. $\mathcal{S}$ explicitly depends on B_x but also implicitly depends on ΔB and B_x through integrals of the crystal amplitude over the shape of the interface. These integrals encapsulate the essence of the coarse-graining procedure. Since the crystal-liquid interface changes nonlinearly, calculating the value of $\mathcal{S}$ requires additional information about the coarse-grained amplitude equations, which is beyond the scope of this study. Here, we check if the $\mathcal{S}$ term has any additional dependence on the noise amplitude N_a. This is not expected for reasonable amounts of noise, since the noise should not change the shape of the interface, only fluctuate it. This is confirmed in Fig. 3, which plots $\mathcal{S}^{-1}$ for different values of N_a and temperature (ΔB). Since $\mathcal{S}$ does not depend on the noise amplitude, one can combine Eqs. (4) and (5) to obtain a quantitative metric of the PFC noise amplitude N_a^2, namely,

$$N_a^2 = \frac{\mathcal{S}}{(\tilde{\gamma}+\tilde{\gamma}'')}. \tag{6}$$

The amplitude N_a can be found from Eq. (6) by computing $\mathcal{S}$ and $(\tilde{\gamma}+\tilde{\gamma}'')$, the latter of which we compute from $\tilde{\gamma}$ for different interface angles in a simulation without added noise (in this process, measuring the exact value of the lattice spacing is essential, as any excess strain needs to be avoided). We note that the metric N_a, assuming the behavior exhibited in Fig. 3, is general and can be applied to any microscopic PFC-type model.

Figure 4 shows the computed results of how N_a depends on the PFC parameters. The left panel shows its dependence on the model's effective temperature ΔB, and the right panel shows its dependence on B_x. It is noteworthy that, within the error bars, N_a depends monotonically on both ΔB and B_x.

Recalling the shape of the noise term from bulk fluctuations, $N_a^2 = 2\Gamma/\bar{\rho}R^d$, and comparing this to the result of Fig. 4 [evaluated via Eq. (6)], we conclude that the product $\bar{\rho}R^d$ needs to depend on the parameters of the PFC free energy expansion to yield quantitative mesoscale fluctuations computed in PFC simulations. In the PFC model, B_x controls the type of material that one models. It is thus not surprising that one needs to constrain the product $\bar{\rho}R^d$ to obtain physically meaningful results.

With ΔB playing the role of temperature in the model, the dependency of $\bar{\rho}R^d$ on ΔB may seem like a surprise at first. We note, however, that the dependency comes purely from the rescaling of the PFC equation of motion. Should the equation be recast into dimensional form, this dependency would disappear, recovering the usual fluctuation-dissipation relation.

This Letter is the first demonstration to show that capturing capillary fluctuations in the PFC simulations quantitatively requires special care to be taken in filtering the noise spectrum and in selecting the noise amplitude in a way that is self-consistently connected with the model parameters of the PFC theory used. Here we computed the self-consistent noise amplitude for the basic PFC model; however, we expect that the approach outlined herein to compute the scaling prefactor N_a of the noise operator in Eq. (3) is generally applicable to all continuum microscopic theories.

This Letter considers the PFC model with Langevin noise as a microscopic theory *in its own right* and examines its long-wavelength behavior. It is unclear if the present model can capture short-scale nonequilibrium fluctuations in a way that is consistent with other microscopic models, such as the one described in Ref. [31]. An upcoming study will examine the statistics of PFC nucleation using the

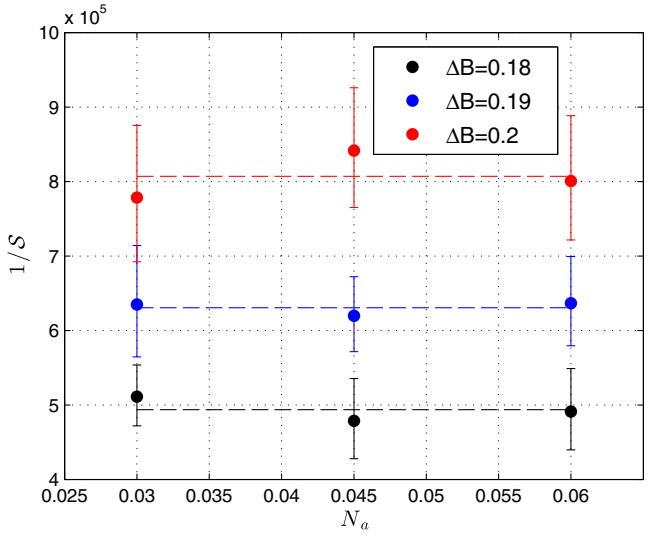

FIG. 3. Prefactor $\mathcal{S}^{-1}$ in the interface power spectrum Eq. (5) versus noise amplitude N_a for different PFC temperature parameters ΔB, with $B_x = 0.7$. The dashed lines are fits.

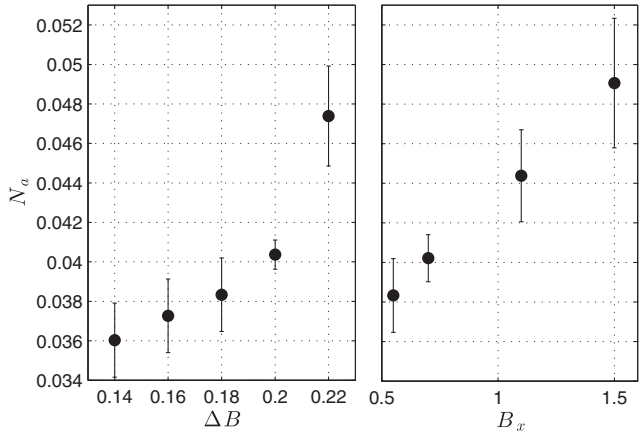

FIG. 4. Computed value of the noise amplitude versus ΔB (left panel, at $B_x = 0.55$) and B_x (right panel, at $\Delta B = 0.18$).

noise properties determined in this work. We note that any type of microscopic PFC-type model could use an approach similar to that presented here to assure agreement with capillary fluctuation theory.

N. P. acknowledges the National Science and Engineering Research Council of Canada for funding and Compute Canada for HPC. N. O.-O. acknowledges the following financial assistance Award No. 70NANB14H012 from U.S. Department of Commerce, National Institute of Standards and Technology as part of the Center for Hierarchical Materials Design (CHiMaD).

[1] K. R. Elder, M. Katakowski, M. Haataja, and M. Grant, Phys. Rev. Lett. **88**, 245701 (2002).
[2] K. R. Elder, N. Provatas, J. Berry, P. Stefanovic, and M. Grant, Phys. Rev. B **75**, 064107 (2007).
[3] H. Emmerich, H. Löwen, R. Wittkowski, T. Gruhn, G. I. Tóth, G. Tegze, and L. Gránásy, Adv. Phys. **61**, 665 (2012).
[4] M. Greenwood, N. Provatas, and J. Rottler, Phys. Rev. Lett. **105**, 045702 (2010).
[5] K.-A. Wu, M. Plapp, and P. W. Voorhees, J. Phys. Condens. Matter **22**, 364102 (2010).
[6] S. K. Mkhonta, K. R. Elder, and Z.-F. Huang, Phys. Rev. Lett. **111**, 035501 (2013).
[7] N. Ofori-Opoku, V. Fallah, M. Greenwood, S. Esmaeili, and N. Provatas, Phys. Rev. B **87**, 134105 (2013).
[8] V. Fallah, A. Korinek, N. Ofori-Opoku, N. Provatas, and S. Esmaeili, Acta Mater. **61**, 6372 (2013).
[9] V. Fallah, A. Korinek, N. Ofori-Opoku, B. Raeisinia, M. Gallerneault, N. Provatas, and S. Esmaeili, Acta Mater. **82**, 457 (2015).
[10] M. Berghoff and B. Nestler, Comput. Condens. Matter **4**, 46 (2015).
[11] J. Mellenthin, A. Karma, and M. Plapp, Phys. Rev. B **78**, 184110 (2008).
[12] J. Berry, N. Provatas, J. Rottler, and C. W. Sinclair, Phys. Rev. B **89**, 214117 (2014).
[13] J. Berry and M. Grant, Phys. Rev. Lett. **106**, 175702 (2011).
[14] A. J. Archer and M. Rauscher, J. Phys. A **37**, 9325 (2004).
[15] Z.-F. Huang, K. R. Elder, and N. Provatas, Phys. Rev. E **82**, 021605 (2010).
[16] Z.-F. Huang, Phys. Rev. E **87**, 012401 (2013).
[17] K.-A. Wu and A. Karma, Phys. Rev. B **76**, 184107 (2007).
[18] S. Majaniemi and N. Provatas, Phys. Rev. E **79**, 011607 (2009).
[19] K.-A. Wu, A. Adland, and A. Karma, Phys. Rev. E **81**, 061601 (2010).
[20] N. Provatas and S. Majaniemi, Phys. Rev. E **82**, 041601 (2010).
[21] A. Adland, A. Karma, R. Spatschek, D. Buta, and M. Asta, Phys. Rev. B **87**, 024110 (2013).
[22] G. I. Tóth, T. Pusztai, G. Tegze, G. Tóth, and L. Gránásy, Phys. Rev. Lett. **107**, 175702 (2011).
[23] S. van Teeffelen, R. Backofen, A. Voigt, and H. Löwen, Phys. Rev. E **79**, 051404 (2009).
[24] L. Gránásy, G. Tegze, G. I. Tóth, and T. Pusztai, Philos. Mag. **91**, 123 (2011).
[25] F. Podmaniczky, G. I. Tóth, T. Pusztai, and L. Gránásy, J. Cryst. Growth **385**, 148 (2014).
[26] B. A. Jugdutt, N. Ofori-Opoku, and N. Provatas, Phys. Rev. E **92**, 042405 (2015).
[27] J. J. Hoyt, M. Asta, and A. Karma, Phys. Rev. Lett. **86**, 5530 (2001).
[28] J. Hoyt, Z. Trautt, and M. Upmanyu, Math. Comput. Simul. **80**, 1382 (2010).
[29] G. I. Tóth, L. Gránásy, and G. Tegze, J. Phys. Condens. Matter **26**, 055001 (2014).
[30] See Supplemental Material at http://link.aps.org/supplemental/10.1103/PhysRevLett.117.220601 for the procedure used to compute the error bars in the Letter.
[31] Q. Bronchart, Y. Le Bouar, and A. Finel, Phys. Rev. Lett. **100**, 015702 (2008).